NASA TM-86677

NASA Technical Memorandum 86677

Transonic Aerodynamic and Aeroelastic Characteristics of a Variable Sweep Wing

P.M. Goorjian, G.P. Guruswamy, H. Ide, and G. Miller

February 1985

National Aeronautics and Space Administration

NASA Technical Memorandum 86677

Transonic Aerodynamic and Aeroelastic Characteristics of a Variable Sweep Wing

P. M. Goorjian, Ames Research Center, Moffett Field, California
G. P. Guruswamy, Informatics General Corporation, Palo Alto, California
H. Ide
G. Miller, Rockwell International, Los Angeles, California

February 1985

National Aeronautics and
Space Administration

Ames Research Center
Moffett Field, California 94035

TRANSONIC AERODYNAMIC AND AEROELASTIC CHARACTERISTICS OF A VARIABLE SWEEP WING

P. M. Goorjian
NASA Ames Research Center, Moffett Field, California 94035, USA

G. P. Guruswamy
Informatics General Corporation, Palo Alto, California 94035, USA

H. Ide
Rockwell International, Los Angeles, California 90009, USA

and

G. Miller
Rockwell International, Los Angeles, California 90009, USA

SUMMARY

The flow over the B-1 wing is studied computationally, including the aeroelastic response of the wing. Computed results are compared with results from wind tunnel and flight tests for both low-sweep and high-sweep cases, at 25.0° and 67.5°, respectively, for selected transonic Mach numbers. The aerodynamic and aeroelastic computations are made by using the transonic unsteady code ATRAN3S. Steady aerodynamic computations compare well with wind tunnel results for the 25.0° sweep case and also for small angles of attack at the 67.5° sweep case. The aeroelastic response results show that the wing is stable at the low sweep angle for the calculation at the Mach number at which there is a shock wave. In the higher sweep case, for the higher angle of attack at which oscillations were observed in the flight and wind tunnel tests, the calculations do not show any shock waves. Their absence lends support to the hypothesis that the observed oscillations are due to the presence of leading edge separation vortices and are not due to shock wave motion as was previously proposed.

1. INTRODUCTION

The variable sweep B-1 wing has been observed to undergo aeroelastic oscillations at certain angles of attack in both flight and wind tunnel tests (Refs. 1 and 2). These oscillations occurred in the transonic regime at both low- and high-sweep angles. Motivated by these observations, in this paper the flow over the B-1 wing is studied computationally, including the aeroelastic response of the wing. Computed results are compared with results from the wind tunnel and flight tests for both the low- and high-sweep cases. In the low-sweep case, the comparisons demonstrate the capability of the computational methods to properly stimulate the flow in the presence of shock waves. In the high-sweep case, where the sweep angle is equal to 67.5°, the comparisons at a low-angle of attack demonstrate the capability of the computational methods to properly simulate the flow at an extreme sweep angle. Finally, a comparison is presented in the high-sweep case for a higher angle of attack at which oscillations were observed. The calculations do not show any shock waves. Their absence lends support to the hypothesis (private communication, Yoshihara, 1984) that the observed oscillations at the high-sweep angle are separation-induced oscillations (SIO). These oscillations are due to the presence of leading-edge separation vortices, and not due to shock-induced oscillations as previously proposed (Ref. 1).

To study the transonic aeroelastic characteristics of wings, efficient computational tools are required to compute unsteady flows over wings. There is an extensive effort in the area of computational fluid dynamics (CFD) (Ref. 3) to develop methods for transonic unsteady aerodynamics. To date methods based on the small disturbance potential theory (Ref. 4) are being routinely used in two-dimensional aeroelastic analysis (Ref. 5). The use of three dimensional methods for practical wings has begun.

An unsteady, small-disturbance transonic code called XTRAN3S that is based on a time-integration method was developed by Borland and Rizzetta (Ref. 6) as an extension to three dimensions. Also this code has the capability of conducting static and dynamic aeroelastic computations by simultaneously integrating the aerodynamic and structural equations of motion. The authors illustrated the capability of XTRAN3S by computing flutter boundaries for a rectangular wing with a 6% thick parabolic-arc airfoil section at transonic Mach numbers. Guruswamy and Goorjian (Ref. 7), and Seidel et al. (Ref. 8) have illustrated the applications to other rectangular wings and Myers et al. (Ref. 9) have illustrated the applications to a transport wing with an aspect ratio of 8, a taper ratio of 0.4, and a leading-edge angle of 20°.

The use of the original version of XTRAN3S was limited to wings with high-aspect ratios, large taper ratios and small sweep angles because of the nature of the coordinate transformation employed. Guruswamy and Goorjian (Ref. 10) developed an alternate efficient coordinate transformation which is incorporated in ATRAN3S. ATRAN3S is a modified version of XTRAN3S with many other new features. As a result, ATRAN3S makes computations faster, more accurate, and more stable than XTRAN3S as is illustrated in Ref. 10 for the F-5 wing, which is a low-aspect, small-taper ratio, high-sweep, fighter wing. An improved version of viscous corrections that were originally implemented in XTRAN3S by Rizzetta and Borland (Ref. 11) are present in

ATRAN3S. The viscous computing capability of ATRAN3S was illustrated by Marstiller et al. (Ref. 12) for a rectangular wing and for a typical transport wing.

In this work, a transonic aeroelastic analysis is conducted for the B-1 wing, which is a variable sweep wing. The sweep angle of the wing varies from 15° to 67.5°, and the aircraft cruises in the transonic regime. Flight tests on the wing and wind tunnel tests (Ref. 2) on the 1/10 scale model of the wing showed angle of attack dependent zero damped aeroelastic oscillations. In a recent aeroelastic model experiment conducted in the NASA Ames 11- by 11-Foot Transonic Wind Tunnel (Ref. 2), significant aeroelastic limited oscillations in the wing-first bending mode were observed in the higher transonic regime over a narrow band of angles of attack. Those oscillations occurred at high-sweep angles of approximately 65°. At the sweep angle of 25°, some small aeroelastic oscillations were also observed, which were attributed to aerodynamic buffeting.

Motivated by these observations, the flow over the B-1 wing is studied computationally, including the aeroelastic response of the wing. The NASA Ames Research Center, transonic, unsteady, code ATRAN3S is used for this purpose. Aerodynamic and aeroelastic analyses are conducted at two sweep angles, 25.0° and 67.5° for selected Mach numbers, and the results are compared with wind tunnel and flight results.

2. AERODYNAMIC EQUATIONS OF MOTION

In this analysis the modified unsteady three-dimensional transonic small-disturbance equation is employed:

$$A\phi_{tt} + B\phi_{xt} = (E\phi_x + F\phi_x^2 + G\phi_y^2)_x + (\phi_y + H\phi_x\phi_y)_y + (\phi_z)_z \tag{1}$$

where ϕ is disturbance velocity potential; $A = M_\infty^2$; $B = 2M_\infty^2$; $E = (1 - M_\infty^2)$; $F = -1/2(\gamma + 1)M_\infty^2$; $G = (1/2)(\gamma - 3)M_\infty^2$; and $H = -(\gamma - 1)M_\infty^2$.

This equation is solved in the computer code ATRAN3S by a time accurate finite-difference scheme that employs an alternating direction implicit (ADI) algorithm (Ref. 4). Whereas ATRAN3S employs the modified coordinate transformation technique (Ref. 10), it is noted here that the conventional transformation originally employed in XTRAN3S (Ref. 6) is not adequate for the high-sweep case of the B-1 wing. During the course of this work, ATRAN3S was further improved by modifying the code to implicitly treat some additional terms in the finite-difference form of Eq. (1) in order to improve the stability of the algorithm. This speeded up the code by a factor of two.

For all cases considered in this study, a grid with 64 points in the streamwise direction, 40 points in the vertical direction and 20 points in the spanwise direction were employed. The wing surface was defined by 39 points in the streamwise direction and by 13 points in the spanwise direction. Computational boundaries were located as follows: the upstream boundary was at 15 chords, the downstream boundary was at 25 chords, the far span boundary was at 1.6 semispans, the region above the wing boundary was at 25 chords, and the boundary below the wing was at 25 chords.

3. AEROELASTIC EQUATIONS OF MOTION

The governing aeroelastic equations of motion of a flexible wing are obtained by the Rayleigh-Ritz method (Chapter 3, Ref. 13). In this method the resulting aeroelastic displacements are expressed at any time as functions of a finite set of assumed modes. The contribution of each assumed mode to the total motion is derived by using Lagrange's equation. Further, it is assumed that the deformation of the continuous wing structure can be represented by deflections at a number of discrete points. This assumption facilitates the use of discrete structural data such as the modal vector, the stiffness matrix and the mass matrix generated that is by a finite element analysis or by experimental influence coefficient measurements.

The final matrix form of the aeroelastic equations of motion is

$$[M]\{\ddot{q}(t)\} + [C]\{\dot{q}(t)\} + [K]\{q(t)\} = \{F(t)\} \tag{2}$$

where

- $[M]$ = the generalized mass matrix
- $[C]$ = the generalized damping matrix
- $[K]$ = the generalized stiffness matrix
- $\{F(t)\}$ = the generalized aerodynamic force vector
- $q(t)$ = the generalized displacement vector
- $\cdot$ denotes the time derivative

These equations of motion are solved numerically by integrating Eq. (2) in time by the linear acceleration method which is the same as the explicit finite difference Euler method. This procedure was successfully employed previously to solve the aeroelastic equations of motion of a two-degrees-of-freedom aeroelastic system (Ref. 5).

The step-by-step integration procedure for obtaining the aeroelastic response was carried out as follows. Free-stream conditions are assumed and wing surface boundary conditions are obtained from a set of selected starting values of the generalized displacement, velocity and acceleration vectors. Then the generalized aerodynamic force vector $\{F(t)\}$ at time $t + \Delta t$ is computed by solving Eq. (1). Using this aerodynamic vector, the generalized displacement, velocity, and acceleration vectors for the time level $t + \Delta t$ are calculated by numerically integrating Eq. (2). From the generalized coordinates computed at the time level $t + \Delta t$, the new boundary conditions on the surface of the wing are computed. With these new boundary conditions the aerodynamic vector $\{F(t)\}$ is computed at the next time level by using Eq. (1). This process is repeated at every time step to solve the aerodynamic and structural equations of motion forward in time until the required response is obtained.

4. MODELING THE WING FOR THE ANALYSIS

A schematic diagram of the B-1 aircraft is given in Fig. 1. From this configuration, isolated wing planforms are modeled to represent the aerodynamic and structural characteristics of the wing as closely as possible. The two planforms modeled for sweep angles of 25.0° and 67.5° are shown in Fig. 2. For both cases, the wing root is located at the pivot point of the wing. The resulting aspect ratio and taper ratio for the 25.0° sweep case are 8.26 and 0.41, and the corresponding values for the 67.5° sweep case are 1.85 and 0.38, respectively.

5. VIBRATIONAL ANALYSIS

In this analysis the assumed modes used in Eq. (2) were taken from the natural modes of the wing as determined from a vibrational analysis. The data for the vibrational analysis was prepared from the measured structural stiffnesses and from the mass distributions of the wing. The first six natural modes were selected to represent the wing for the aeroelastic analysis. The modes and their associated frequencies that were determined by the vibrational analysis in addition to the frequencies of the actual wing from ground vibration tests of the B-1 aircraft are given in Fig. 3. The frequencies from the vibration analysis on the model planform of the wing that are prepared for the code are close to those measured for the actual wing in the ground vibration test as shown in Fig. 3. Thus the model in the code closely represents the structural characteristics of the actual wing.

6. STEADY AERODYNAMIC ANALYSIS

Steady aerodynamic computations were made in order to verify that the modeling of the wing was adequate for representation of the actual aerodynamic characteristics of the wing. This verification was made by comparing the results from ATRAN3S with the wind tunnel results measured at the NASA Ames 11- by 11-Foot Tunnel on a 1/10-scale model of the wing (Ref. 2).

Steady aerodynamic pressures were computed by integrating Eq. (1) in time and by setting the steady boundary conditions on the wing. The time-step size required for the computation depended mainly upon the sweep angle. The time-step sizes required for the 25.0° and the 67.5° sweep cases were 0.01 and 0.002, respectively.

Steady-state computations were made for subsonic and transonic Mach numbers equal to 0.65 and 0.75, respectively, at the sweep angle of 25°. Steady pressure distributions are compared with experiment at four semispan stations along the sections perpendicular to the elastic axis at 46, 61, 72, and 83% locations. Figure 4 shows the steady pressure distribution at $M = 0.65$ and $\alpha = 0.0°$ where the flow is subsonic. As expected the ATRAN3S results compare well with experiment. Figure 5 shows the comparison of steady pressure distributions at $M = 0.75$ and $\alpha = 4.11°$. Results compare well between the code and the experiment for all span stations. These close comparisons between the code and the experiment show that the planform modeled in Fig. 2 for the sweep of 25° is adequate to aerodynamically represent the wing.

Steady-state computations were then made for several Mach numbers ranging from 0.80 to 0.873 at various angles of attack for the sweep angle of 67.5°. The physical grid required to make computations is shown in Fig. 6. Note the scale in the span direction was stretched by a factor of ten in Fig. 6a in order to show the details of the grid. In the actual grid, the wing appears swept back by 67.5° as shown in Fig. 6b. It is noted here that the physical grid generated by the original XTRAN3S (Ref. 7) is not adequate (Ref. 10) for this high-sweep case. Because of the high sweep and the associated low Mach numbers normal to the leading edge, the flow remained subsonic for all the cases considered. The code compared fairly well with the experiment at small angles of attack. For example, Fig. 7 shows steady pressure comparisons between the code and the experiment at four semispan stations along sections perpendicular to the elastic axis at 46, 61, 72, and 83% locations at $M = 0.873$ and $\alpha = 2.06°$. Comparisons are favorable for all span stations except the 46% semispan station. The disagreement at the 46% semispan is due to the presence of the glove close to that span station in the wind tunnel tests and the glove is not modeled in the code.

For the high-sweep angle of 67.5°, at higher angles of attack, both in flight tests and in wind tunnel tests, the wings were observed to undergo oscillations (Refs. 1 and 2). For the flight tests, the oscillations occurred in the range of 8.1-8.4° in angle of attack, and for the wind tunnel tests the oscillations occurred at 7.44°. It had been proposed in Ref. 1 that the oscillations were due to the motion of shock

waves. However, upon examination of the wind tunnel detail (Refs. 1 and 2), which included pressure coefficient plots, oil flow charts, and lift curve slopes, H. Yoshihara (private communication, 1984) suggested that the oscillations were due to "the presence of leading-edge separation vortices modified by secondary separation effects." Furthermore, the oscillations could be explained by the following mechanism: "Here wing bending (primary mode) leads to outboard washout changes that cause vortex-flow loading changes (180° out of phase) that reinforce the bending oscillations."

To determine whether shock waves were contributing to the oscillation, calculations were performed at $M = 0.80$ and at $\alpha = 6.0°$ and $11.0°$ angles of attack. At these angles of attack, the wind tunnel data showed no oscillations, and the calculations should indicate the presence of shock waves if they are there. However, the code ATRAN3S models the flow by a velocity potential as shown in Eq. (1), and hence cannot account for the presence of vortices in the flow. Figure 8 shows the comparison at $\alpha = 6.0°$ between wind tunnel test results and calculations. The calculations show no sign of the presence of shock waves and differ significantly from the experimental results. Note that the experimental data falls below C_p^*. Figure 9 shows the computed results at $\alpha = 11.0°$. Again there is no sign of the presence of shock waves and the results differ significantly from the experimental results shown in Fig. 9. Hence there are probably no shock waves present at the intermediate angle of attack of 7.44° at which the oscillations were observed. To properly model the flow in these cases, where leading edge vortices are apparently present and the effects of separation are important in understanding the oscillations, a Navier-Stokes code must be used.

7. AEROELASTIC RESPONSES

In this section several calculations will be presented that simulate the aeroelastic response of the wing by simultaneously integrating Eqs. (1) and (2). The first case will examine the response of the wing at low sweep under the subsonic flow conditions given in Fig. 4. A transonic case will then be computed at the low-sweep angle to determine the presence of shock waves. Finally a subsonic case will be computed at the high-sweep angle, under the flow conditions given in Fig. 7, to examine the change in the response of the wing as the sweep angle is increased.

For the first case, an aeroelastic analysis is conducted at the subsonic Mach number of 0.65 and $\alpha = 0.0°$ in order to study the nature of subsonic response of the wing. In this case the steady pressures from the code compared well with the experiment as shown in Fig. 4. Flow parameters are taken for an altitude of 33,000 ft. The response computations were initiated by giving an arbitrary unit displacement to the first generalized coordinate $q(1)$. The aerodynamic and structural equations of motion were simultaneously integrated forward in time until a steady aeroelastic equilibrium state was approached. This required about 10,000 time-steps of size 0.02, which corresponds to approximately 6 sec of physical time at the altitude of 33,000 ft.

In order to simulate an external disturbance to initiate oscillations, an instantaneous change of 2.0° to the mean angle of attack was given to the wing and the response computations were further continued. After initial oscillations the wing again approached a steady aeroelastic equilibrium position. This required approximately 5,000 time-steps. Similar responses were repeated for 4.0° of instantaneous change in the angle of attack. These responses for the first normal mode are shown in Fig. 10. The responses for the other 5 modes were of smaller amplitude in comparison to the first mode. For all the three instantaneous angles of attack, the wing reached a steady aeroelastic equilibrium position within approximately 3.5 sec.

For the next case, the response analysis was conducted for the transonic flow at $M = 0.72$ and $\alpha = 4.0°$ and an altitude of 33,000 ft. At these conditions some oscillations were observed in the flight test of the B-1 aircraft (Refs. 1 and 2). Response computations were initiated by giving an arbitrary unit displacement to the first generalized coordinate $q(1)$. Then aerodynamic and structural equations of motion were simultaneously integrated in time until a steady aeroelastic equilibrium state was approached. This required about 10,000 time-steps of size 0.02, which corresponds to 6 sec of physical time at the altitude of 33,000 ft. The response time was similar to the subsonic case. The deformed shape of the wing at its steady aeroelastic equilibrium position is shown in Fig. 11. This deformed shape of the wing is close to the first bending mode shape of the wing. The corresponding upper- and lower-surface pressure distributions are shown in Fig. 12. A shock wave is evident on the outboard portion of the upper surface of the wing.

To simulate an external disturbance to initiate oscillations, an instantaneous change in the mean angle of attack was given to the wing and response computations were further continued. After some initial oscillations, the wing again approached a steady aeroelastic equilibrium position within 3.0 sec. This required approximately 5,000 time-steps. Such responses were conducted for two instantaneous changes in angle of attack of 2.0° and 4.0°. These responses are shown for the first normal mode in Fig. 13. For the two cases, the wing reaches a steady aeroelastic equilibrium position within approximately 3.0 sec.

In spite of the presence of shock waves on the wing, the nature of response is similar to that observed for the subsonic case at $M = 0.65$. It is noted that the wing does not pick up oscillations caused by the external disturbance even when shock waves are present on the wing. However, these calculations did not simulate the effects of the shock wave interaction with the boundary layer. Hence they could not simulate buffet, which was the cause of the oscillations that were observed in wind tunnel and flight tests (Refs. 1 and 2) at these flow conditions.

For the final computation, a case at $M = 0.873$ and $\alpha = 2.06°$ was selected for response analysis at the altitude of 33,000 ft. For this case steady pressures from ATRAN3S compared favorably with the experiment as shown in Fig. 7.

Because of the low aspect ratio of 1.8 of the wing at the 67.5° sweep-case, the time-step size required was 0.002, which is ten times smaller than the time step size required for the 25.0° sweep case. Because of the large computational time required for the aeroelastic analysis, only a limited response analysis was conducted. The aeroelastic response of the first normal mode is shown in Fig. 14 for approximately two cycles of oscillation starting from the free-stream conditions with an initial unit value for the first generalized displacement q(1). The response computations which corresponds to 1.35 sec of physical time required about 15,000 time-steps of computation. The response showed damping but at a very small rate. The rate of damping for this case is much smaller than those observed for the case of 25.0° sweep. This small damping, in addition to the proposed formation of leading-edge vortices at higher angles of attack might have caused the aeroelastic oscillations that were observed on the B-1 wing at the high-sweep angle.

8. CONCLUSION

The transonic code ATRAN3S was used to study the aerodynamic flow and the aeroelastic response of the B-1 wing at low- and high-sweep angles of 25.0° and 67.5°, respectively. Steady pressures from the code compared well with experimental results in the low-sweep case for both subsonic and transonic flows. At high sweep, the comparisons were good at low angles of attack. But at higher angles of attack, the calculations did not show shock waves as had been previously proposed. An alternative source for the oscillations that were observed at the higher angles of attack is proposed to be leading-edge separation vortices. A Navier-Stokes code is required to properly simulate such flows. Aeroelastic response studies showed that the damping of the wing response significantly decreased when the sweep angle was increased. The calculations using ATRAN3S were performed on a CRAY X-MP computer and they required 0.46 sec of CPU time to calculate one time step for a total of 1.9 hr of CPU time for one complete aeroelastic response analysis for a low-sweep case.

REFERENCES

1. Stevenson, J. R., "Shock Induced Wing Oscillation Wind Tunnel Test Results," Aerospace Flutter and Dynamics Council Conference, Williamsburg, Va., April 4-6, 1984.

2. Dobbs, S. K. and Miller, G. D., "Self Induced Oscillation Wind Tunnel Test of a Variable Sweep Wing," (to be presented at the AIAA 26th Structural Dynamics Conference, Orlando, Fla., April 1985).

3. Goorjian, P. M., "Computations of Unsteady Transonic Flows." In Recent Advances in Numerical Methods in Fluids, Vol. IV. Advances in Computational Transonic, ed. W. G. Habashi, Pineridge Press Ltd., U.K., 1984.

4. Ballhaus, W. F. and Goorjian, P. M., "Implicit Finite Difference Computations of Unsteady Transonic Flows About Airfoils," AIAA J., Vol. 15, Dec. 1977, pp. 1728-1735.

5. Guruswamy, P. and Yang, T. Y., "Aeroelastic Time Response Analysis of Thin Airfoils by Transonic Code LTRAN2," Computers and Fluids, Vol. 9, No. 3, Dec. 1980, pp. 409-425.

6. Borland, C. J. and Rizzetta, D. P., "Transonic Unsteady Aerodynamics for Aeroelastic Applications, Volume I--Technical Development Summary for XTRAN3S," AFWAL-TR-80-3107, June 1982.

7. Guruswamy, P. and Goorjian, P. M., "Comparison Between Computational and Experimental Data in Unsteady Three Dimensional Transonic Aerodynamics Including Aeroelastic Applications," AIAA Paper 82-0690-CP, May 1982.

8. Seidel, D. A., Bennett, R. M., and Ricketts, R. H., "Some Recent Applications of XTRAN3S," NASA TM 85641, May 1983.

9. Myers, M. R., Guruswamy, P., and Goorjian, P. M., "Flutter Analysis of a Transport Wing Using XTRAN3S," AIAA Paper 83-0922, May 1983.

10. Guruswamy, P. and Goorjian, P. M., "An Efficient Coordinate Transformation Technique for Unsteady Transonic Aerodynamic Analysis of Low Aspect Ratio Wings," AIAA Paper 84-0972-CP, 25th AIAA Structural Dynamics Conference, Palm Springs, May 1984.

11. Rizzetta, D. P. and Borland, C. J., "Numerical Solution of Three-Dimensional Unsteady Transonic Flow Over Wings, Including Inviscid/Viscous Interaction," AIAA Paper 82-0352, Jan. 1982.

12. Marstiller, J. W., Guruswamy, P., Yang, T. Y., and Goorjian, P. M., "Effects of Viscosity and Modes on Transonic Flutter Boundaries of Wings," AIAA Paper 84-0870-CP, 25th AIAA Structural Dynamics Conference, Palm Springs, Calif., May 1984.

13. Bisplinghoff, R. L., Ashley, H., and Halfman, R. L., "Aeroelasticity." Addison Wesley, Menlo Park, Calif., Nov. 1957.

ACKNOWLEDGMENT

We would like to thank Dr. H. Yoshihara for his helpful comments on interpreting the experimental data and acknowledge his introduction of the concept of separation-induced oscillations (SIO), i.e., the presence of leading edge separation vortices modified by secondary separation effects as being the source of the oscillations that were observed to occur on the wing in the high sweep case.

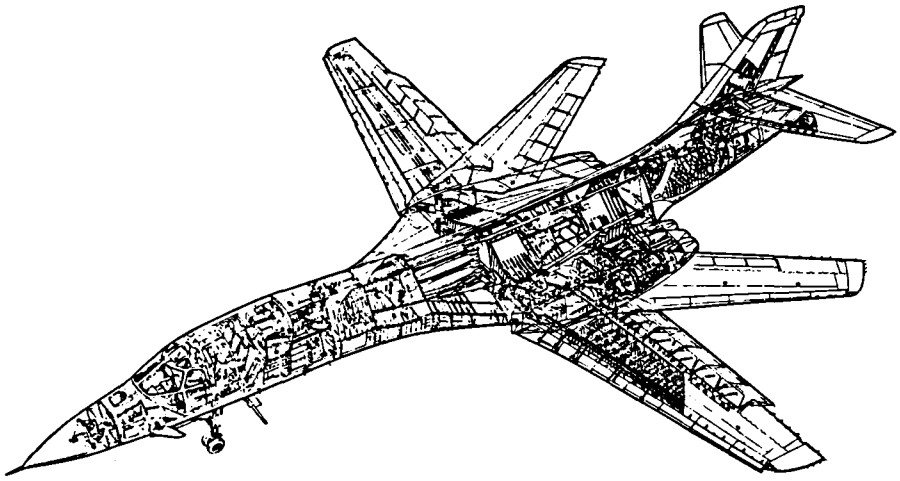

Fig. 1. The B-1 aircraft.

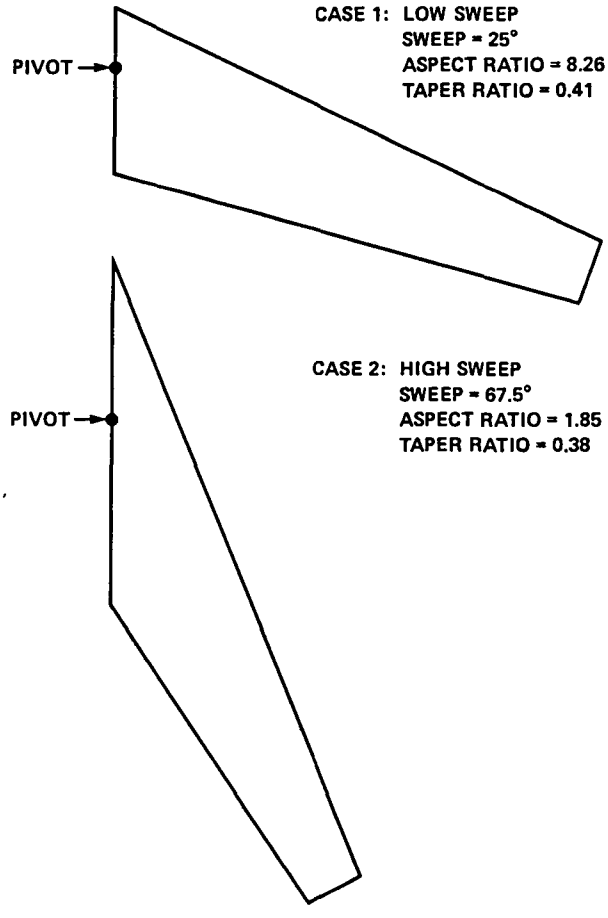

Fig. 2. Wing planforms for analysis.

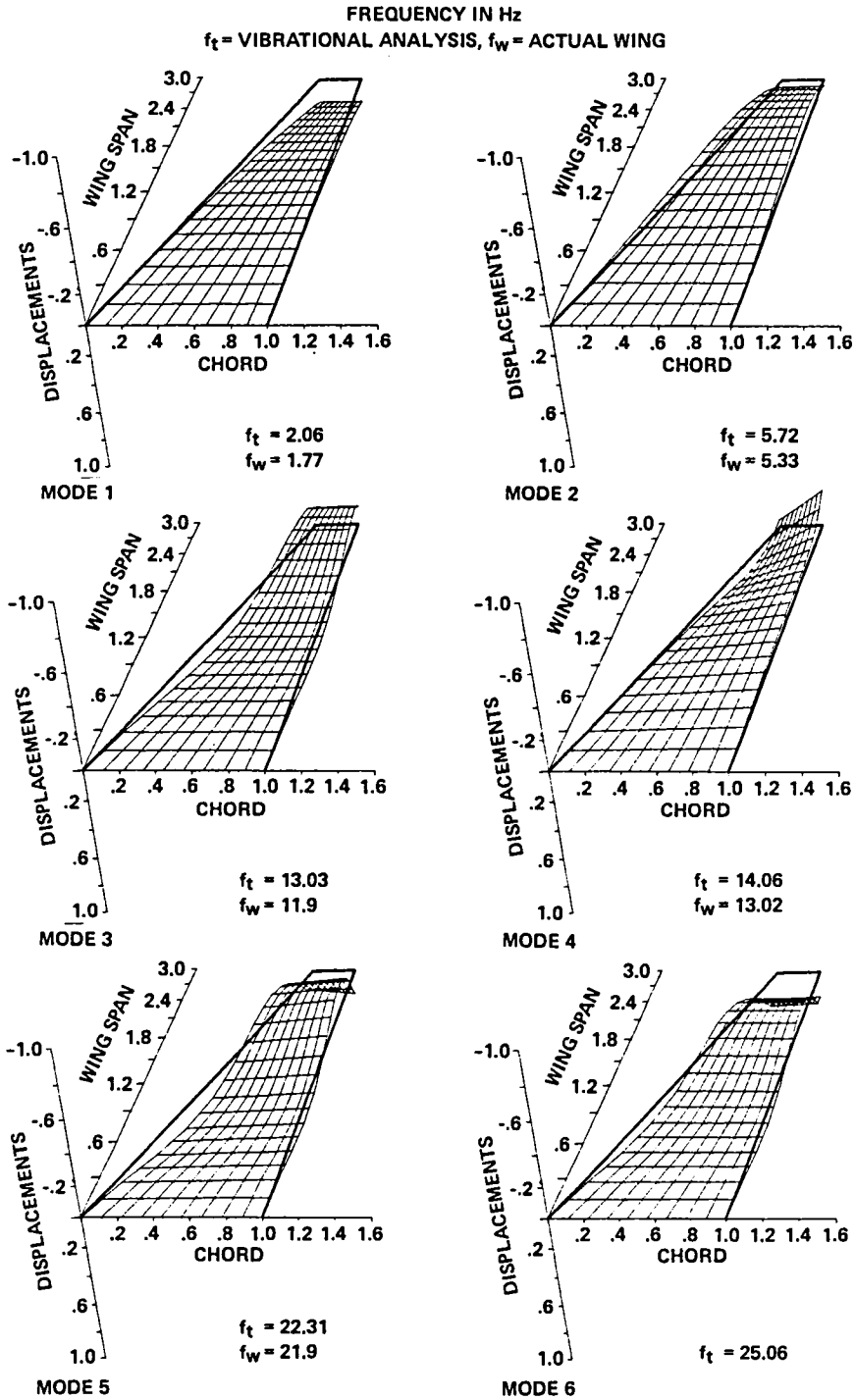

Fig. 3. Six natural vibration modes.

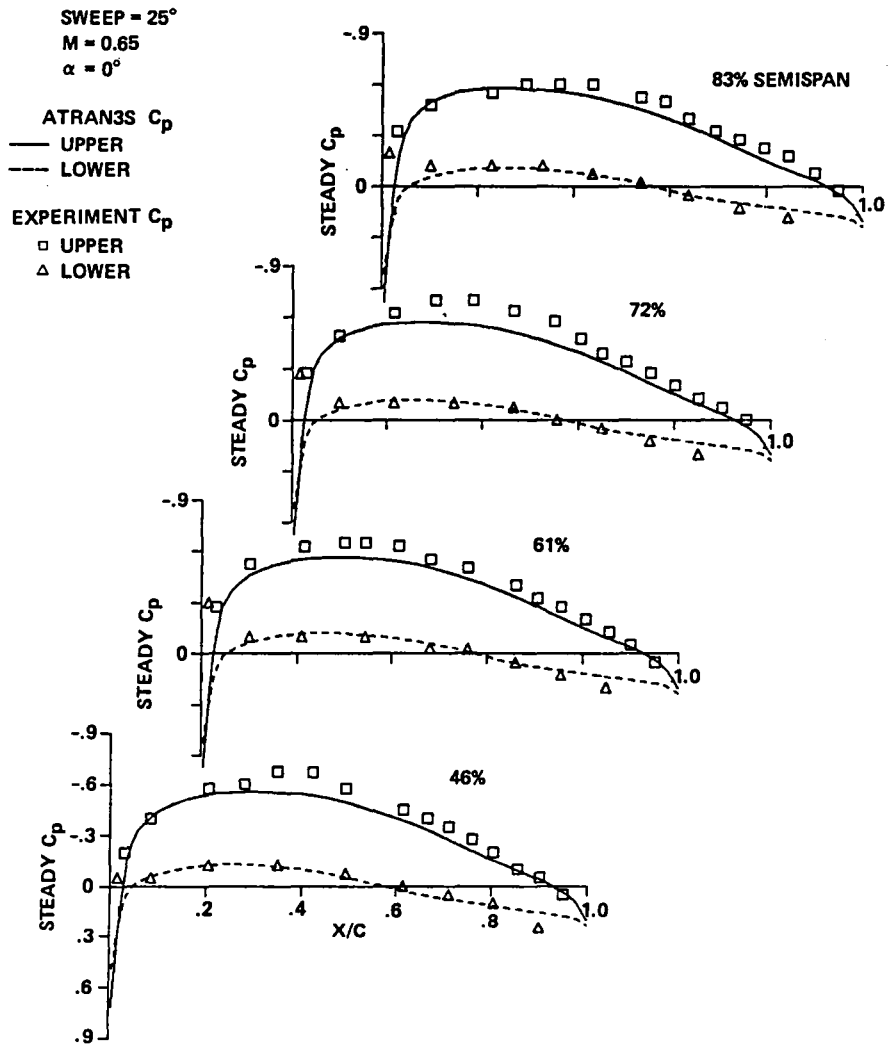

Fig. 4. Steady pressure distributions for the 25° sweep case at $M_\infty = 0.65$.

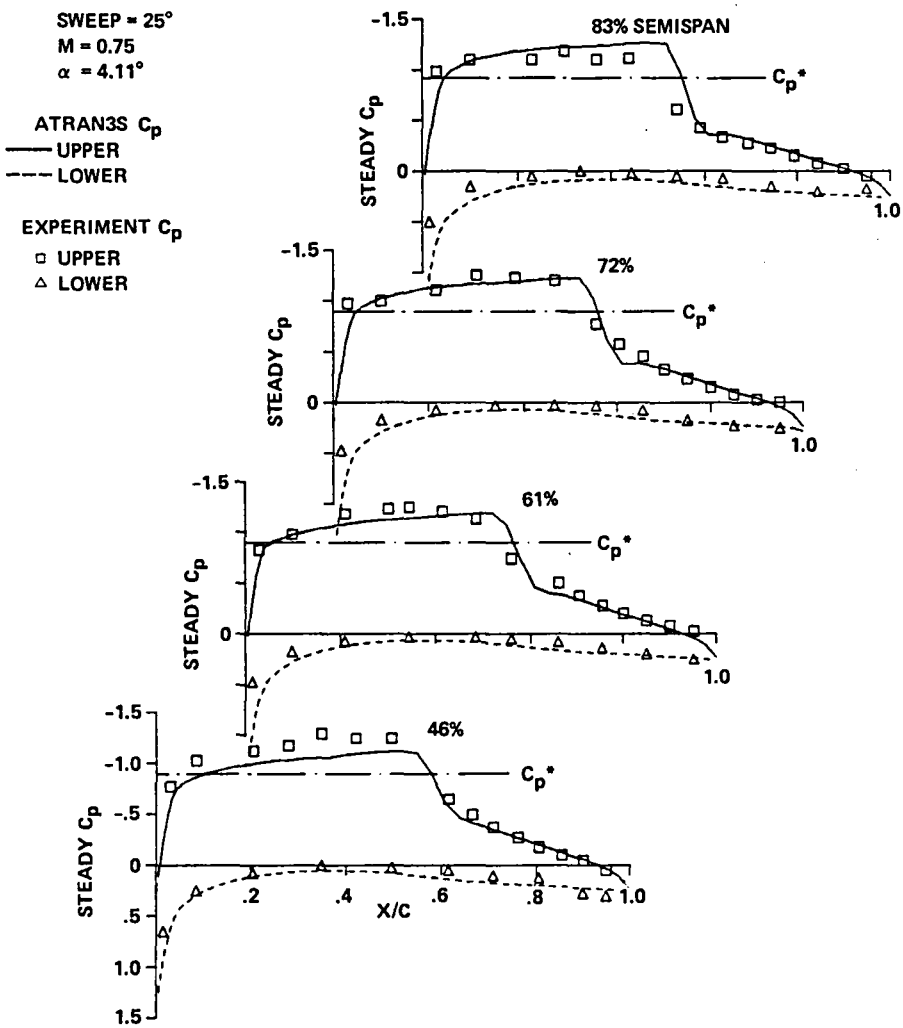

Fig. 5. Steady pressure distributions for the 25° sweep case at $M_\infty = 0.75$.

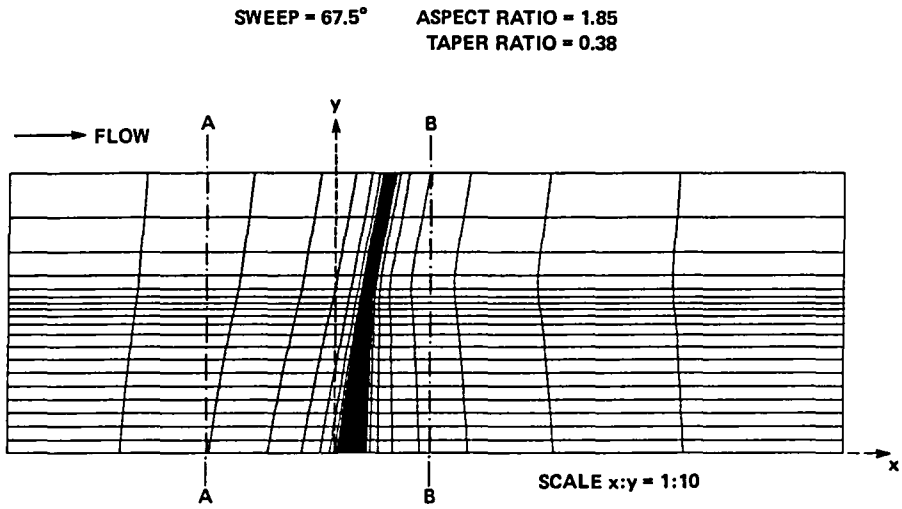

(a) Full grid.

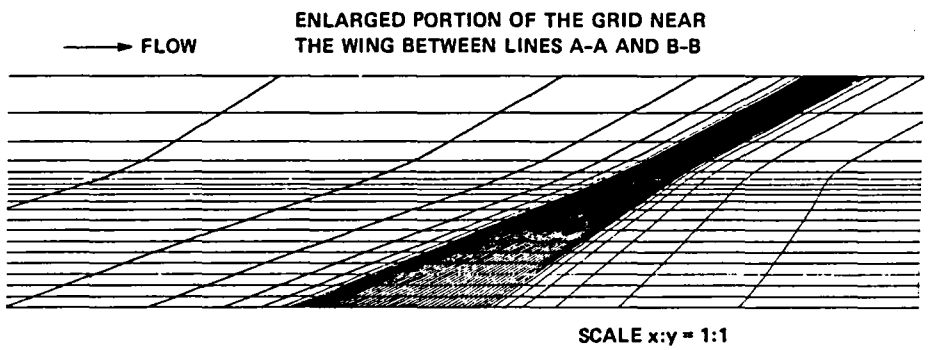

(b) Blow up near wing.

Fig. 6. Physical grid for the 67.5° sweep case.

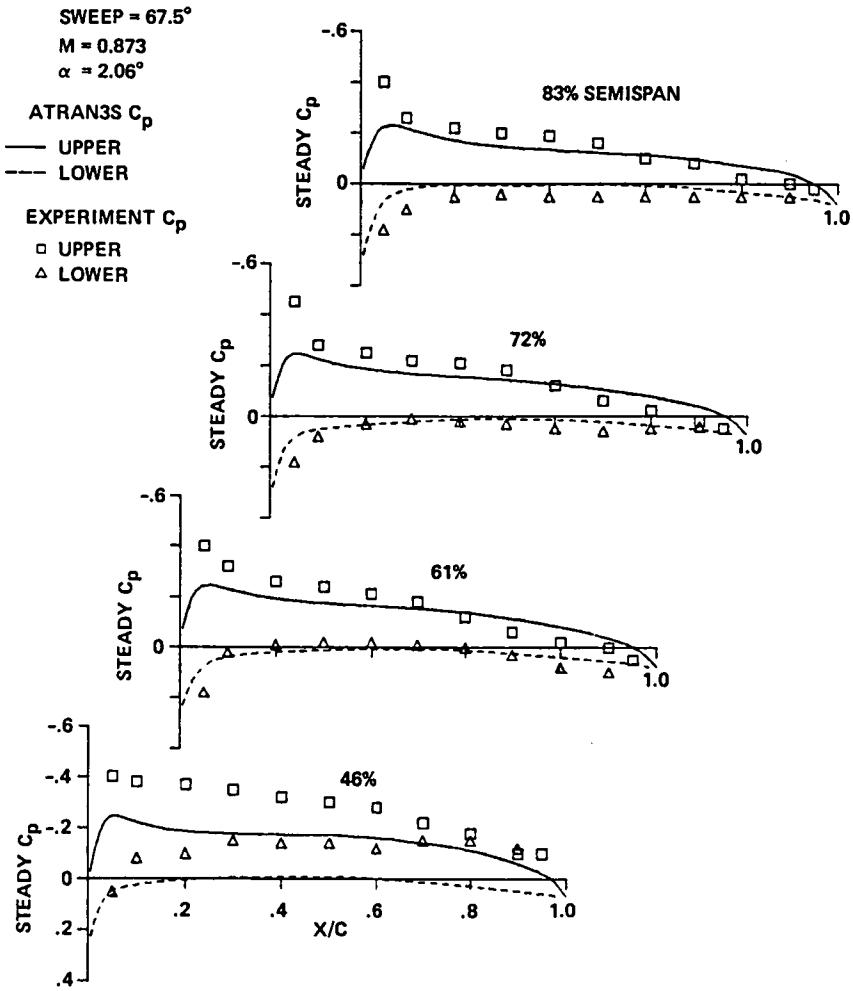

Fig. 7. Steady pressure distributions for the 67.5° sweep case at $M_\infty = 0.873$ and $\alpha = 2.06°$.

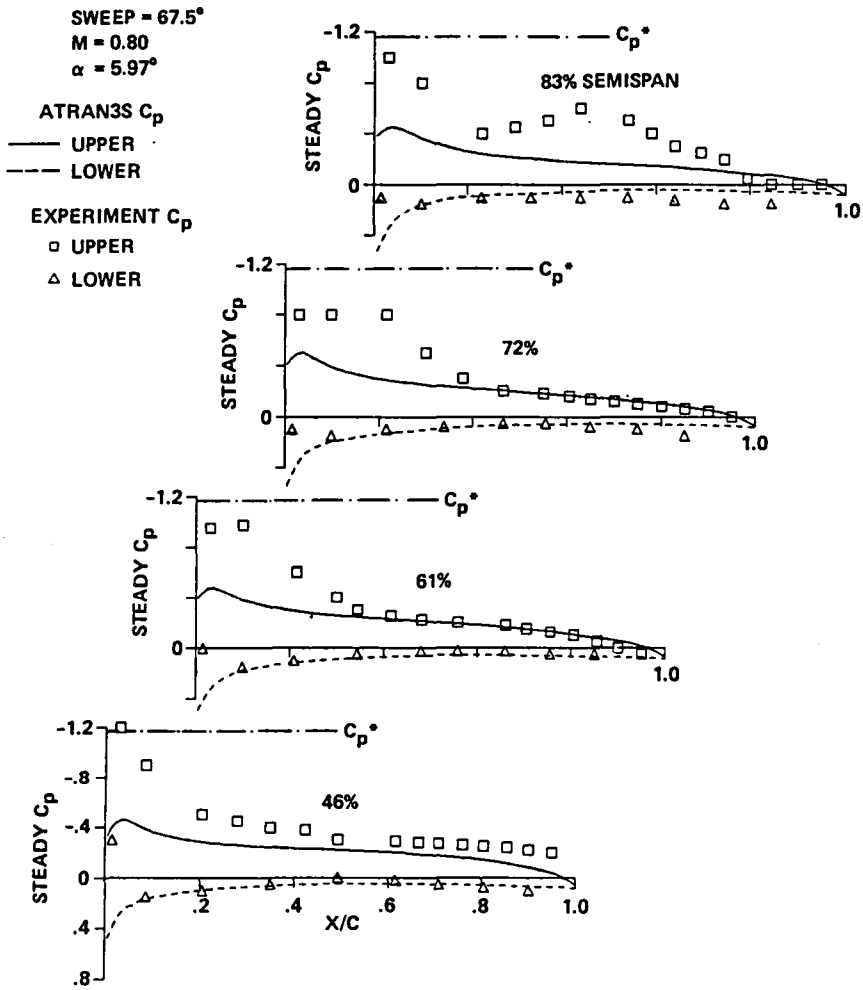

Fig. 8. Steady pressure distributions for the 67.5° sweep case at $M_\infty = 0.80$ and $\alpha = 5.97°$.

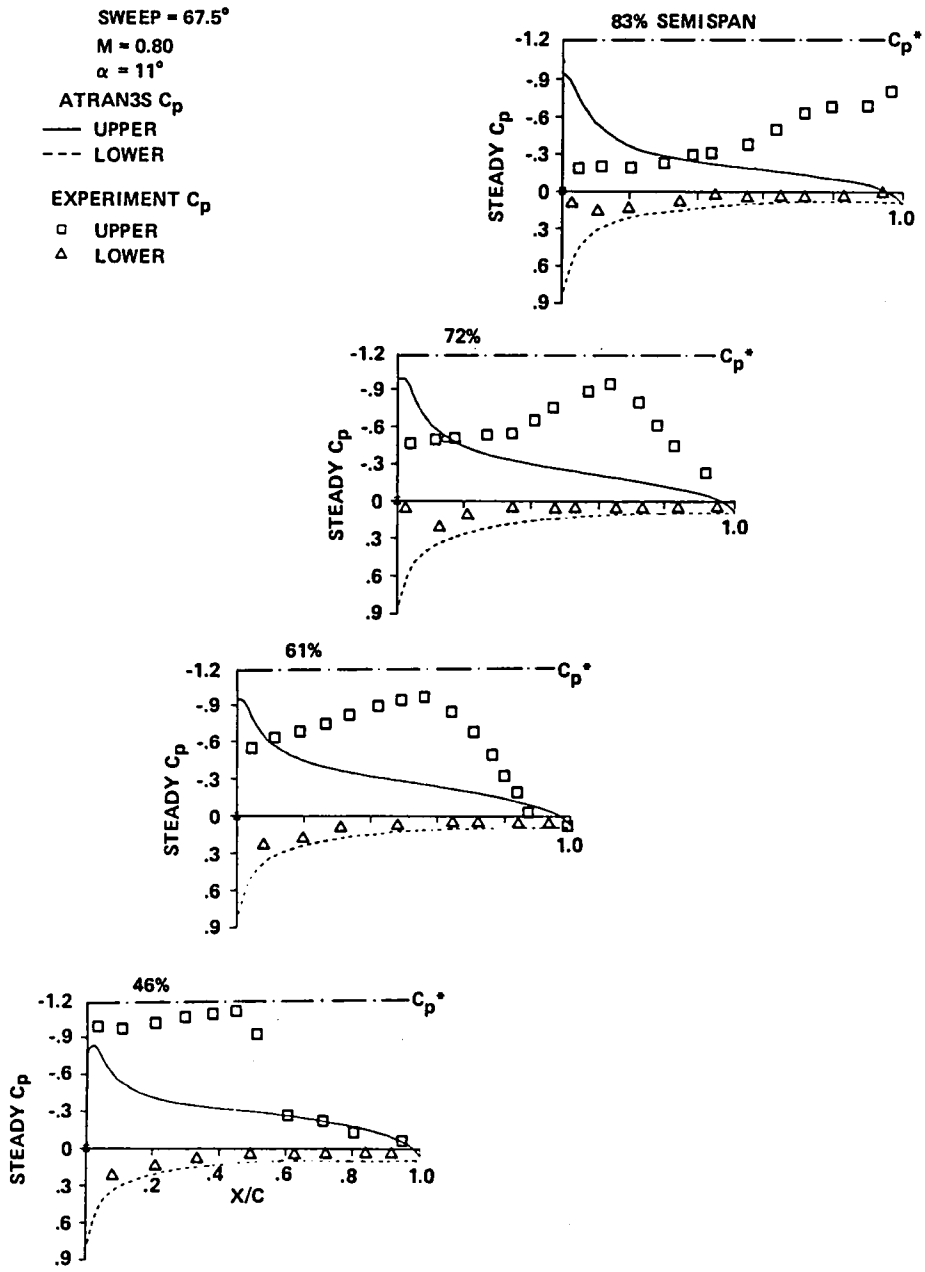

Fig. 9. Steady pressure distributions for the 67.5° sweep case at $M_\infty = 0.80$ and $\alpha = 11.0°$.

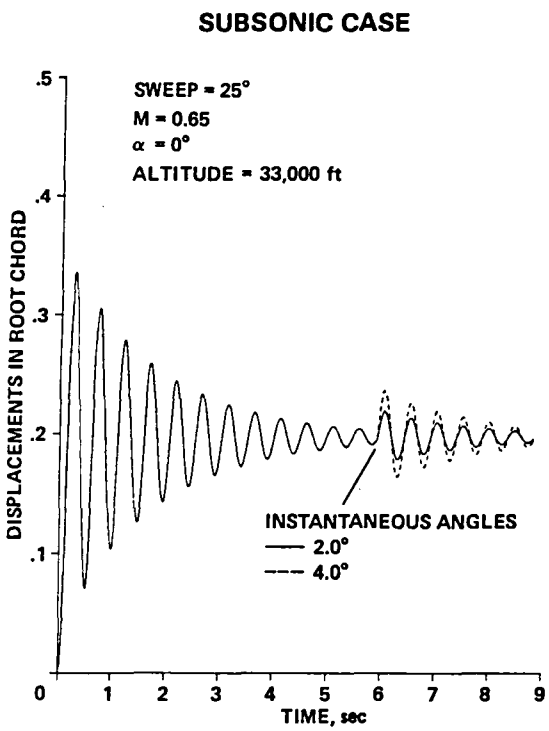

Fig. 10. Dynamic aeroelastic responses of the first normal mode for the 25° sweep case at M = 0.65.

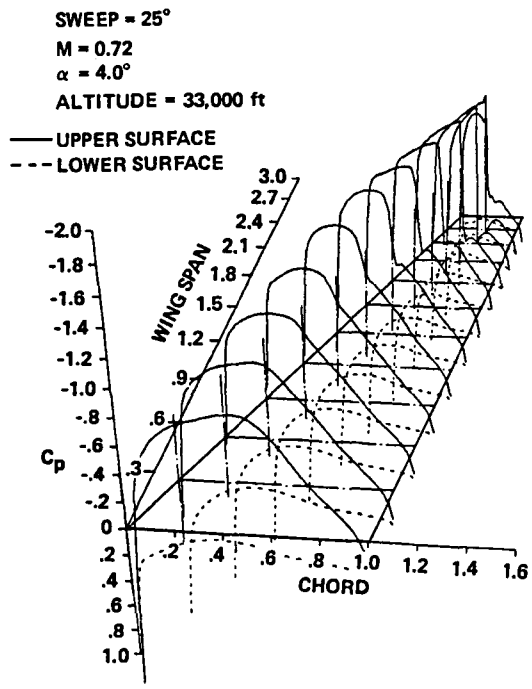

Fig. 12. Pressure distributions at the static aeroelastic equilibrium position.

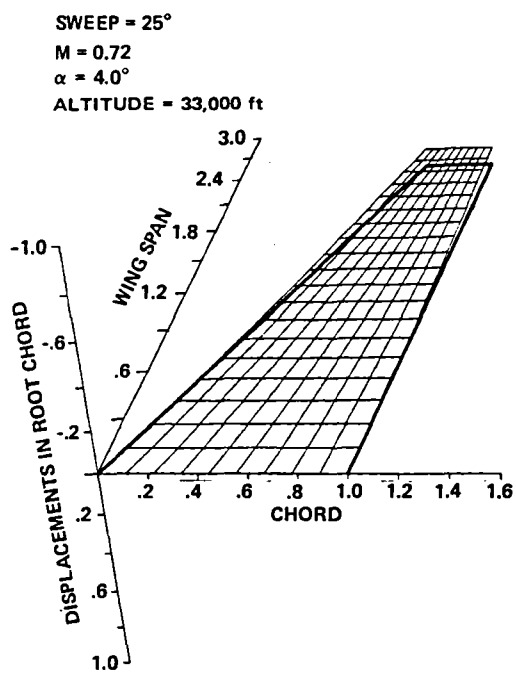

Fig. 11. The deformed shape at the static aeroelastic equilibrium position.

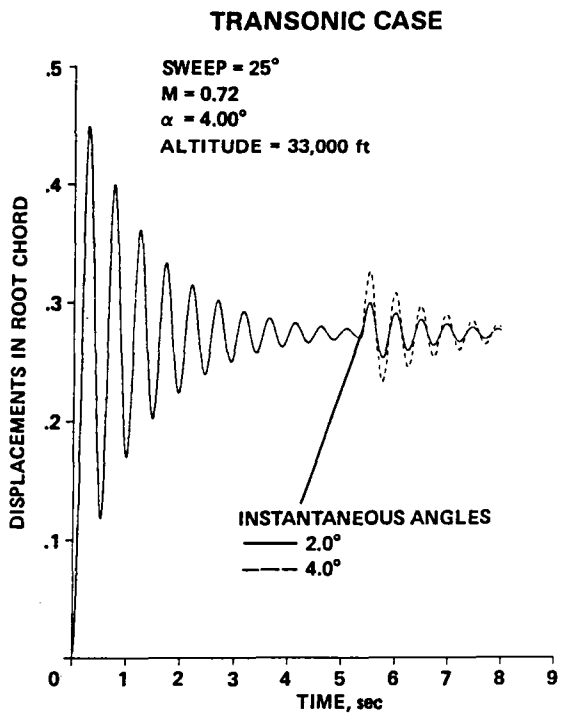

Fig. 13. Dynamic aeroelastic responses of the first normal mode for the 25° sweep at M_∞ = 0.72.

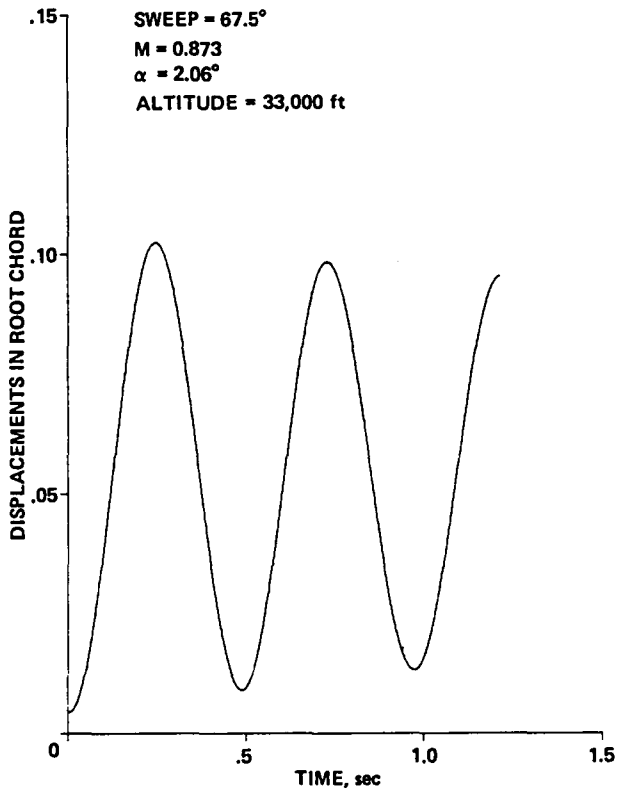

Fig. 14. Dynamic aeroelastic response of the first normal mode for the 67.5° sweep at $M_\infty = 0.873$.

1. Report No.	2. Government Accession No.	3. Recipient's Catalog No.
NASA TM-86677		

4. Title and Subtitle	5. Report Date
TRANSONIC AERODYNAMIC AND AEROELASTIC CHARACTERISTICS OF A VARIABLE SWEEP WING	February 1985
	6. Performing Organization Code

7. Author(s)	8. Performing Organization Report No.
Goorjian, P. M, Guruswamy, G. P. (Informatics General Corp., Palo Alto, Calif.), and Ide, H. and Miller, G. (Rockwell International, Los Angeles, Calif.)	85119
	10. Work Unit No.

9. Performing Organization Name and Address	11. Contract or Grant No.
NASA Ames Research Center Moffett Field, Calif. 94035	
	13. Type of Report and Period Covered
12. Sponsoring Agency Name and Address	Technical Memorandum
National Aeronautics and Space Administration Washington, D.C. 20546	14. Sponsoring Agency Code 505-31-01-01-00-21

15. Supplementary Notes

Point of Contact: Peter Goorjian, Ames Research Center, MS 202A-14, Moffett Field, Calif. 94035 (415) 694-5547 or FTS 464-5547

16. Abstract

The flow over the B-1 wing is studied computationally, including the aeroelastic response of the wing. Computed results are compared with results from wind tunnel and flight tests for both low-sweep and high-sweep cases, at 25.0° and 67.5°, respectively, for selected transonic Mach numbers. The aerodynamic and aeroelastic computations are made by using the transonic unsteady code ATRAN3S. Steady aerodynamic computations compare well with wind tunnel results for the 25.0° sweep case and also for small angles of attack at the 67.5° sweep case. The aeroelastic response results show that the wing is stable at the low sweep angle for the calculation at the Mach number at which there is a shock wave. In the higher sweep case, for the higher angle of attack at which oscillations were observed in the flight and wind tunnel tests, the calculations do not show any shock waves. Their absence lends support to the hypothesis that the observed oscillations are due to the presence of leading edge separation vortices and are not due to shock wave motion as was previously proposed.

17. Key Words (Suggested by Author(s))	18. Distribution Statement
Unsteady aerodynamics Aeroelasticity Transonic flow	Unlimited Subject category - 02

19. Security Classif. (of this report)	20. Security Classif. (of this page)	21. No. of Pages	22. Price*
Unclassified	Unclassified	19	A02

*For sale by the National Technical Information Service, Springfield, Virginia 22161

End of Document